Supporting Information

Hill et al. 10.1073/pnas.1202128109

SI Materials and Methods

Circuit Building. Model microcircuits were built using the BlueBuilder application described elsewhere (1). The locations of the somata were assigned randomly within their layer boundaries. The corresponding 3D morphologies were then loaded at these locations, and a touch detection algorithm was run to detect all structural appositions for all neurons in the circuit.

Touch Detection. To account for bouton swelling and spine extension, any axodendritic apposition less than 2.5 μm was considered a potential connection (unless otherwise specified; i.e., if the axon of neuron i came at least one time within 2.5 μm of the dendrite of neuron j, i was said to be structurally connected to j).

The 3D neuron morphologies, obtained through Microbrightfield's Neurolucida (compare with 3D reconstruction), are composed of thousands of consecutive small cylinders, where each cylinder is equivalent to one sample point from the reconstructor along that neural process. Hence, detecting an axodendritic apposition is equivalent to performing what is referred to in computer graphics as a cylinder to cylinder collision (with cylinders' radii augmented with one-half the max spine length). The number of cylinder–cylinder collisions tests to be performed is equal to the number of axon segments multiplied by the number of dendrite segments for all of the circuit, a huge number given the scale of the circuits that we are simulating.

Therefore, we have devised an algorithm that efficiently examines all possible dendrite and axon touches. By dividing the volume of the circuit into voxels containing an equivalent number of neurite segments and running cylinder–cylinder collision for each voxel in parallel on separate processors, we parallelized the touch detection step and dramatically reduced the run time. The algorithm was run on an IBM BlueGene/P supercomputer with 16,384 processors.

Density Computation. The density of the axon or dendrite is computed from its 3D representation consisting of a set of small cylinders typically 1–5 μm long (depending on the discretization done by the reconstructer). The soma of the neuron is placed at the center of a 3D grid, and the dimension of each voxel is $50 \times 50 \times 50$ μm. The volume of each cylinder is computed and added to the voxel containing the cylinder's center.

Axodendritic Convolution. The value of convolution of the dendritic and axonal density profiles is computed by overlaying the centered axonal density map with the dendritic density map; the former is centered at voxel v. The value of the convolution map at voxel v is then the sum over the whole map of the product of the axon density and dendrite density at each voxel in that configuration. The same is repeated for each voxel v to obtain a complete convolution map.

1. Sfyrakis K, et al. (2006) *FENS* Abstr., Vol 3, A037.16.

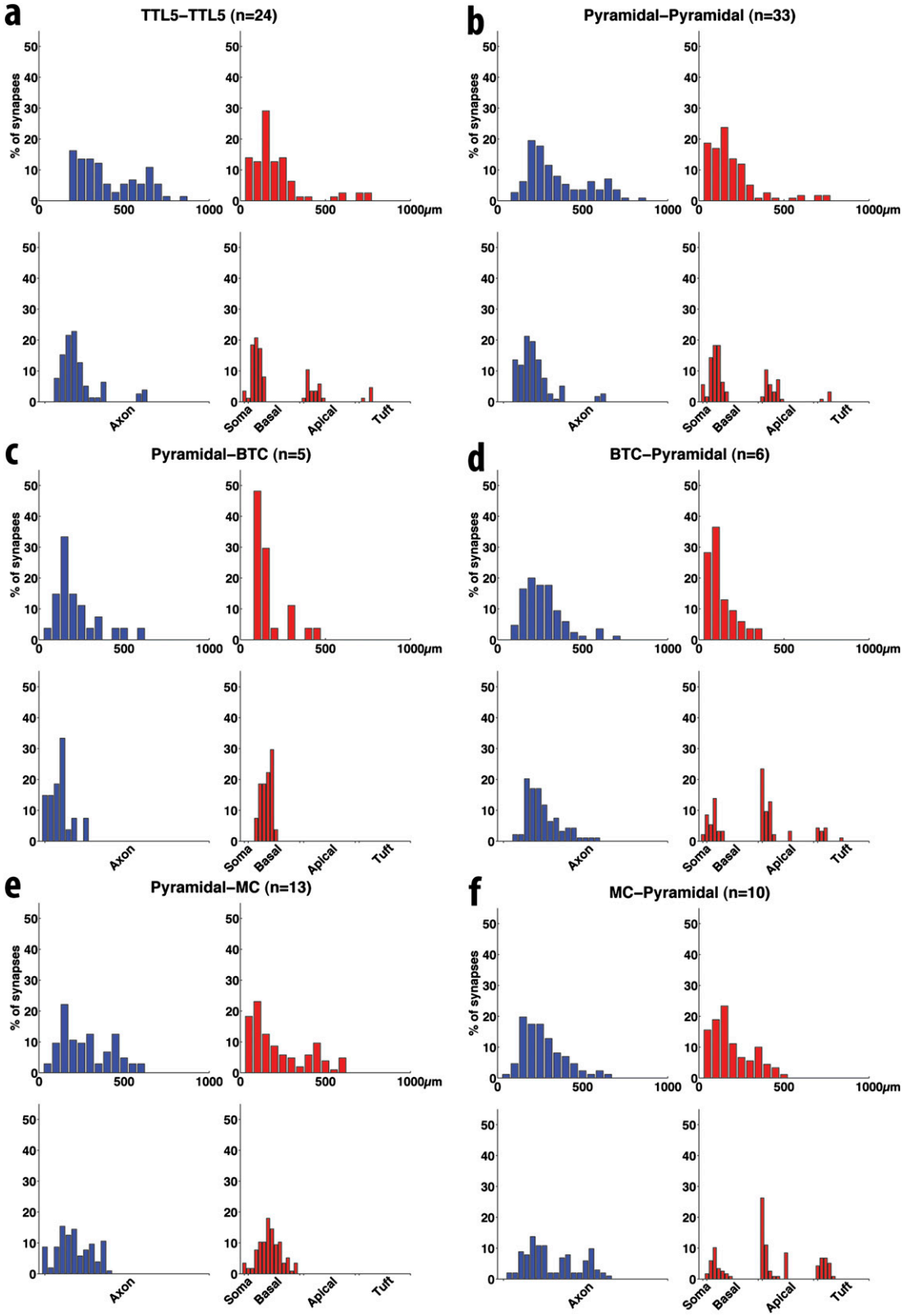

Fig. S1. Functional innervation patterns in in vitro neocortical microcircuitry. The measured functional innervation patterns according to both path distance from the soma (*Upper*) and branch order (*Lower*) between (*A*) thick-tufted layer 5 (TTL5) pyramidal cells (PCs), (*B*) all PCs (composition in Table 1), (*C*) PC to bitufted cell (BTC), (*D*) BTC to PC, (*E*) PC to Martinotti cell (MC), and (*F*) MC to PC. In each panel, the blue graph indicates the presynaptic innervation pattern on the axon, and the red graph indicates the postsynaptic innervation pattern on the dendrite.

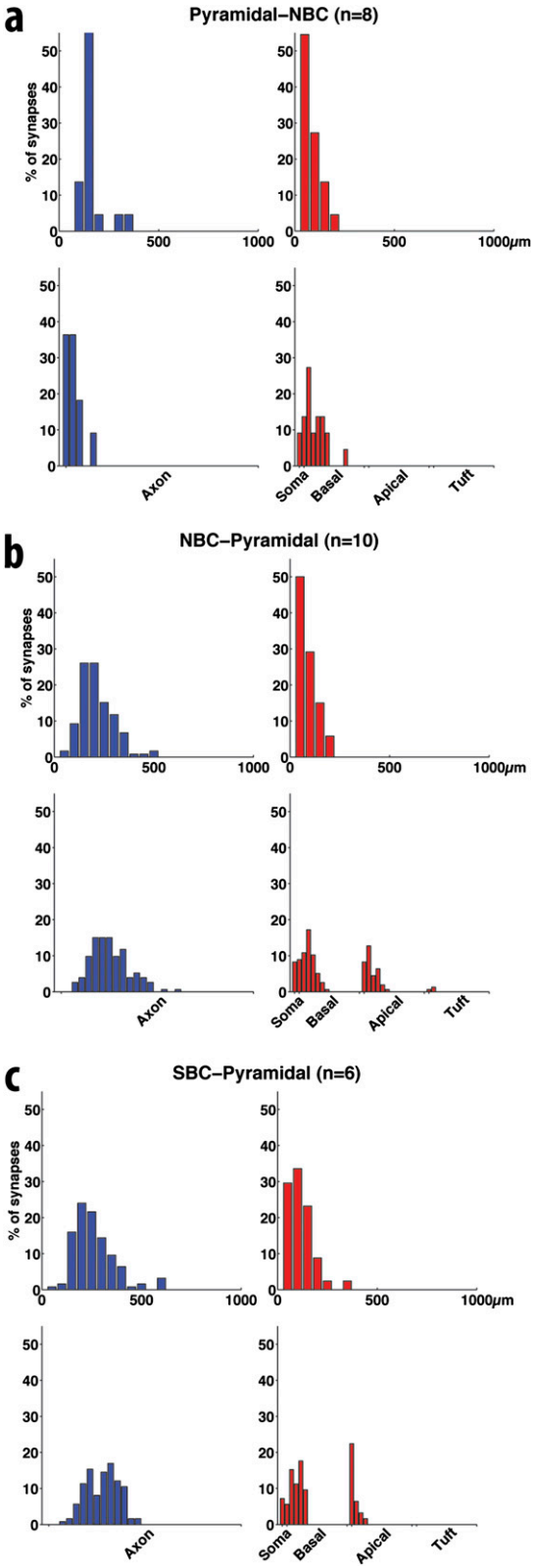

Fig. S2. The same as Fig. S1 but for (*A*) PC to nest basket cell (NBC), (*B*) NBC to PC, and (*C*) SBC to PC.

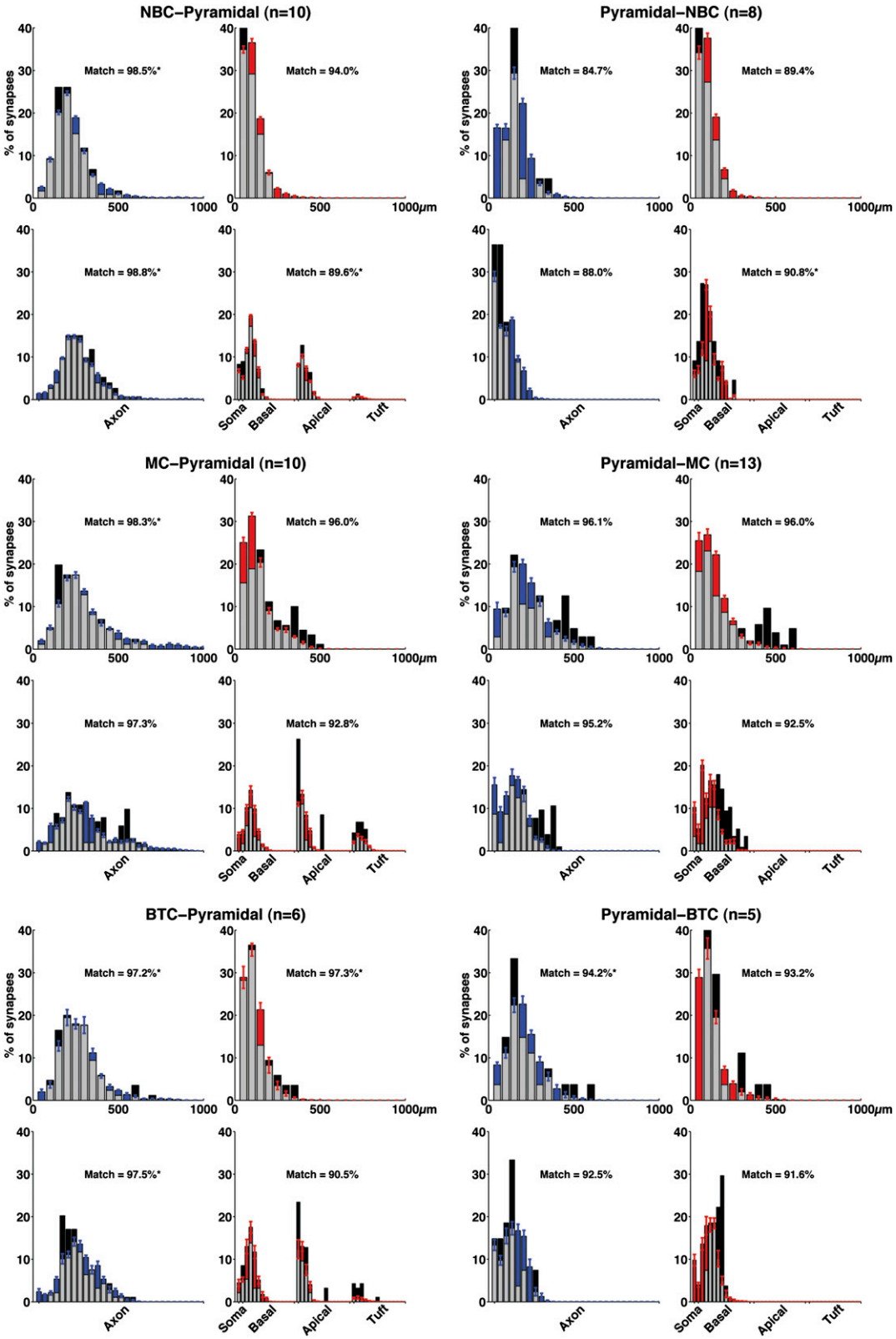

Fig. S3. Comparison of functional and structural innervation patterns for different connection types. The color coding is the same as in Fig. 3. Both path distance and branch order innervations are shown. Histograms of mean ± SEM locations are shown between NBC and PC, MC and PC, and BTC and PC.

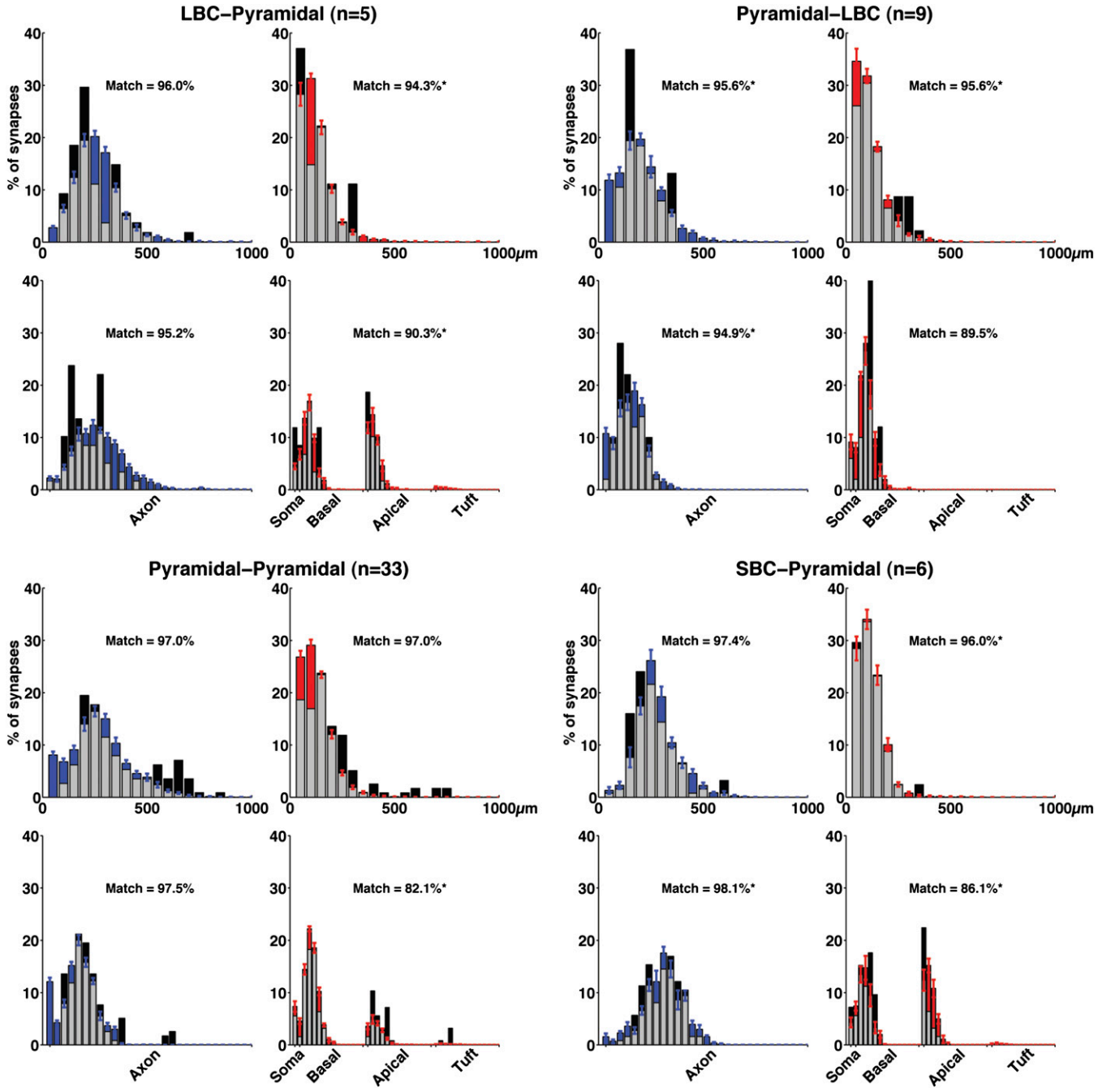

Fig. S4. Comparison of functional and structural innervation patterns for different connection types. The same as in Fig. S3 but for large basket cells (LBCs) and PCs, PCs, and small basket cells (SBCs) to PCs.

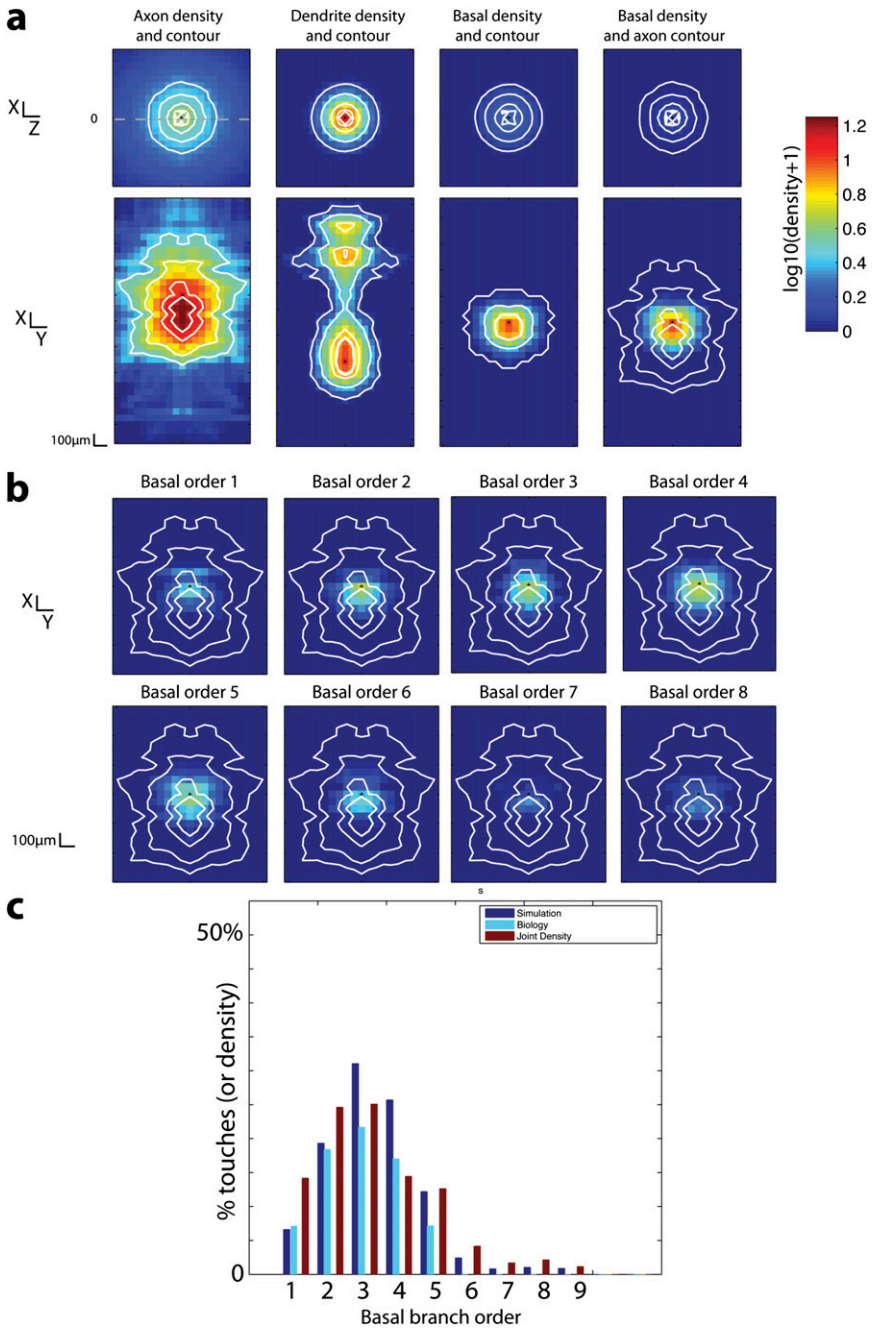

Fig. S5. Derivation of pyramidal neuron basal innervation from morphological density. (*A*) Soma-centered density representations of axons of TTL5 neurons (n = 24) were computed for the entire axon and the entire apical and basal dendrites. Then, we computed the density caused by only the basal dendrite fibers and overlaid the contour of the axon for visualization purposes. (*B*) We separated the density of each basal branch order (1–8) and computed the joint density ($d_{axon} \times d_{basal}$) over all voxels. (*C*) Therefore, we estimated the percentage of synapses formed on each portion of the neuron. The joint density formed a distribution with the same characteristic shape of the biological data and data from a model microcircuit composed of the same neurons.

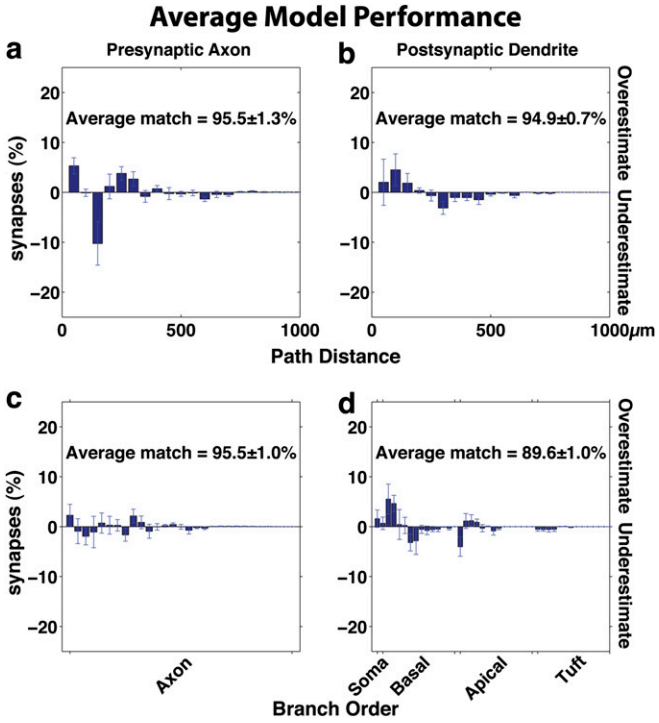

Fig. S6. Average model performance over all pathways. (*A*) The mean ± SEM percentage synapses that are over- or underestimated for the presynaptic axon and (*B*) postsynaptic dendrite according to path distance from the soma and (*C* and *D*) the branch order.